NIFS--88

JP9109091

High Resolution Spectroscopy of H^+ Energy Loss in Thin Carbon Film

N. Matsunami and K. Kitoh

(Received – May 7, 1991)

NIFS-88 May 1991

High Resolution Spectroscopy of H^+ Energy Loss in Thin Carbon Film

Noriaki Matsunami and Kenshin Kitoh

Crystalline Materials Science,
Faculty of Engineering, Nagoya University

Furo-cho, Chikusa-ku, Nagoya 464-01, Japan

Abstract

The energy loss of ~100 keV H^+ transmitted through thin carbon film of 7 nm has been measured with the resolution of ~20 eV. We have observed new energy loss peaks around 210 and 400 eV in addition to the normal energy loss peak around 1 keV. We find that the experimental artifacts, ionization of C K-(290 eV) and impurity inner-shells, extreme non-uniformity of films, events associated with elastic scattering are not responsible for these peaks. The origin of these low energy loss peaks will be discussed.

Key words : Proton energy loss, New peak, Carbon film,
Plasma excitation, High resolution

1 Introduction

Excitation of plasmons by electrons has been observed and recognized as an elementary excitation in solids for more than twenty years [1] and is reviewed in a recent article [2]. However, plasmon excitation by heavy ions has not been observed yet, probably due to the severe requirement that the energy resolution be 10 eV for ions of the energy more than several 10 keV per nucleon.

In this paper, we have measured the energy loss spectrum of ~100 keV H^+ in ~7 nm carbon films by means of proton energy loss spectroscopy with a resolution of ~20 eV [3-5]. We have observed new energy loss peaks at 400 and 210-230 eV in addition to the normal energy loss peak at ~1 keV. Experimental artifacts, C K- and impurity inner-shell ionization, extreme non-uniformity of films, events associated with some elastic scatterings are examined and we find that none of these is responsible for the new energy loss peaks. The origin of the new energy loss peaks, especially the 210 eV peak, is discussed.

2 Experimental

The details of the experimental apparatus have been reported elsewhere [3-5] and a brief description is given here. Protons generated with a hollow cathode ion source are accelerated to a voltage V_a. After bended by a magnet, the proton beam is deflected by 12° with an electrostatic field as shown in Fig. 1. Protons transmitted through a carbon film supported on copper mesh are decelerated by V_a-V_o, V_o being the offset voltage so that only protons of the final energy E_f=1 keV can pass through the electrostatic analyzer and be detected with a secondary electron multiplier. The energy loss ΔE is given by

$$\Delta E=qV_o-E_f \quad , (1)$$

where q is the proton charge. We obtain the energy loss spectrum by varying the offset voltage. The beam size was ~1 mm^2 and a typical current was 1 nA. The pressure of the sample chamber was $\sim 10^{-7}$ Torr. The arc discharge method was used to prepare the carbon films. The C-film/Cu mesh assembly could be moved so that the energy loss without and with C-film can be measured without changing any condition. Fig. 2 shows the energy loss distribution without C-film for 100 keV H^+. The energy resolution in this case was 24 eV. The zero energy loss was also determined to an accuracy of a few eV. In Fig. 2, we see no structure, i.e., flat spectrum except for zero energy loss peak.

3 Experimental Results

The energy loss distributions of H^+ transmitted through carbon films are shown in Fig. 3(a) and (c) for 100, and (b) and (d) for 120 keV. The nominal thickness determined by the crystal thickness monitor is ~1.5 $\mu g/cm^2$ or ~7 nm, assuming the density of $N=11.3 \times 10^{22}/cm^3$ (2.25 g/cm^3). We see the normal energy loss peak at ~1 keV as estimated by the stopping power of S_e=165 and 156 eV/nm for 100 and 120 keV H^+, respectively [6,7]. The most probable energy loss ΔE_p indicated by arrows in the figure was used to determine the film thickness: 6.1, 6.1, 7.3 and 7.7 for Fig. 3(a) to (d) and the error is estimated to be 10 %, including several % shift of ΔE_p due to ion bombardment[8]. The spectra of Fig. 3(a) and (b) were obtained for the same film, but the films for Fig. 3(a), (c) and (d) were different with each other. The normal energy loss peaks are fitted by an asymmetric Gaussian as expected [9,10], the half-width being indicated by the numbers in the figure. The experimental mean half-width of 0.82 in Bohr units for Fig. 3(a) is in reasonable agreement with the theoretical estimates of 0.89[11].

It is noted that a peak at 400 eV is seen for as prepared samples shown by the crosses in Fig. 3(c) and (d), after subtracting the asymmetric Gaussian of the normal energy loss peak. Surprisingly, the 400 eV peak disappears after H^+ bombardment of relatively small dose of $\sim 0.1\ \mu C/mm^2$ as shown by open circles in Fig. 3(a) and (b). In addition, we see a weak but non negligible peak at 210-230 eV, which was relatively insensitive to H^+ bombardment, in the expanded energy loss spectra for $\Delta E \leq 300$ eV. No peak was observed due to single plasmon excitation at 25 eV, whose value was measured by 200 keV e impact on 21 nm film. The fact that no peak has been observed other than the zero energy loss peak for the Cu mesh without a C-film as in Fig. 2 excludes the possibility that the experimental artifacts are the origin of the new energy loss peaks.

Impurities in the C-film are now considered. 2 MeV He^+ Rutherford backscattering (RBS) of C-film (~10 nm) on Be substrate shows no detectable impurities (<a few %) of heavier elements, except for oxygens which are present in Be substrate, as seen in Fig. 4. From these spectra, the concentrations of impurities having the binding energy of ~210 eV such as B, S, and Cl were estimated to be less than 0.7, 0.3 and 0.3 %, respectively. Elastic recoil detection (ERD) by 1.5 MeV He^+ shows ~10 % H in the C-film of 40 nm. This amount of H contributes to the stopping power by 3 %[6,7].

Obviously, the new energy loss peaks differ from ionization of the C K-shell with the binding energy of 290 eV [12], which was not observed. In Table 1, we list the possible impurities having the inner shell binding energy of ~210 eV[12], the ionization cross section[13], ionization probability for ℓ=6 nm and necessary impurity concentration giving rise to the observed 210 eV peak intensity of 10^{-3}. Here 2 and

6 electrons are used for s and p shell ionization, respectively. This and RBS results described earlier lead to the conclusion that the inner-shell ionization of impurities can not explain the new peak. Similarly, the 400 eV peak is not ascribed to the inner shell ionization.

The possibility of extreme non-uniformity of the film is also unlikely, because these low energy loss peaks appear at almost the same position for different films. The result of 120 keV H^+ in Fig. 3(b), which was obtained using the same position of the same film as Fig. 3(a), shows the peak at the same value of 210 eV. This result rules out the possibility that the peaks are associated with some scattering events, because the peak energy should shift in proportion to the incident energy, if it is the case (see Fig. 3(a) and (b)).

Similar spectra are also obtained for different film thickness. In Fig. 5, the ratio of the peak intensity around 210 eV over the normal peak intensity is plotted against ΔE_p or the film thickness. We see the oscillatory behaviour of the 210 eV peak intensities.

4. Discussion

The 400 eV peak is sensitive but 210 eV peak is insensitive to ion bombardment. Hence the origin of the two peaks would be different. The channeling effect could be a candidate for the 400 eV peak. However, the film is unlikely to be a good crystal but more likely to be amorphous. The origin of the 400 eV peak is not understood at present.

The 210 eV peak is sharp and weak. The integrated peak area over the normal energy loss peak is $\sim 10^{-3}$. Excitations of the electron-hole (e-h) pairs should produce a broad peak similar to the normal peak. A candidate for a sharp energy loss peak is multi-plasmon excitations. We examine the possibility that the multi-plasmon peak is isolated from

the mixture of the e-h pair and plasmon excitations which generate the broad peak or the normal energy loss peak.

One recalls that the density fluctuation of plasmon is coherent and very different from that of e-h pair excitations. Thus, there would be interference between plasmon and e-h pair excitations, because incoherency may destroy coherency. Moreover, according to the electron density fluctuation equation [1], the plasmon is well defined only if the average charge density of the valence electrons responsible for the plasmon is canceled out by the positive charge, i.e., only if the charge neutral condition is satisfied during time Δt and space $\Delta \ell$ relevant to plasmon excitation. The presence of charge such as electrons and holes during the characteristic time and space will break the charge neutrality condition. These arguments lead to that protons can excite either plasmon or e-h pair at a time and that once a plasmon excitation occurs, there is no electronic excitation during Δt, which is supposed to be of order of the plasmon oscillation period,

$$\Delta t \sim 2\pi/\omega_p \quad , \tag{2}$$

where ω_p is the plasmon frequency. Note that $\Delta t \sim 10^{-16}$ s is larger by an order of magnitude than the excitation time $\hbar/\Delta E \sim 10^{-17}$ s, $\hbar$ and ΔE being the Planck constant and the excitation energy. This, called the exclusive excitation hypothesis, states that protons with the velocity v travel by the characteristic length λ_o without any excitation after plasmon excitation

$$\lambda_o \simeq \Delta t \, v \quad . \tag{3}$$

This hypothesis reveals inevitably the *correlation* between successive excitations, depending on the electronic excitation strength. This is very important for the present case because zero energy loss peak has not been observed, i.e., the probabilities of no excitation are very

small or practically zero. The simplest correlation which can produce the isolated multi-plasmon peak is given by

Prob.{plasmon ->plasmon, plasmon ->e-h, e-h ->plasmon, e-h ->e-h}

$$=\{P_o,\ 1-P_o,\ 0,\ 1\}. \qquad (4)$$

This means that the probability of the plasmon excitation after plasmon excitation is P_o and e-h pair after plasmon is $1-P_o$. The plasmon after e-h would be small(0), because the coherent density fluctuation would not be easily produced after incoherent density fluctuation.

The above argument finally leads to the following equation.

$$\ell = n\lambda_o + x\lambda_e \quad , \qquad (5)$$

where ℓ is the film thickness, n is an integer, λ_e is the mean free path for e-h pair excitation and x is a real number. The energy loss ΔE is written as

$$\Delta E = n\hbar\omega_p + x\bar{T} \quad , \qquad (6)$$

where $\bar{T}$ is the mean energy of e-h pair excitation. When the film thickness is appropriate so that x is zero, there would appear the multi-plasmon peak with the intensity of P_o^n. Isolation of this peak from the mixture of e-h pair and plasmon excitations and general features of the energy loss are demonstrated by a simulation calculation as in Fig. 6. In the calculation, C K-shell contribution was neglected. We used that $\hbar\omega_p$=26 eV and λ_o=0.75 nm(c.f., $2\pi v/\omega_p$=0.73 nm) for plasmon excitation, and T^{-2} distribution with T_{min}=20 eV, T_{max}=220 eV ($\bar{T}$=53 eV) and the mean free path=$\exp(-\ell_e/\lambda_e)$ with λ_e=0.3 nm for e-h pair excitations. We assume that P_o=0.5 or equal probabilities of plasmon and e-h pair excitations and the initial probability of plasmon excitation =P_o. In Fig. 6(a) for ℓ=6 nm, the well-isolated multi-plasmon peak of n =8 is seen at 208 eV as well as the normal energy loss peak at ~ 1 keV. The calculated peak intensity is 4×10^{-3} which is comparable with the

experimental value of $\sim 10^{-3}$. As the film thickness increases, the multi-plasmon peak diminishes (Fig. 6(b),(c)) and the multi-plasmon of n =9 with weaker intensity appears again at ΔE=234 eV for t=6.75 nm. This oscillatory behaviour of the peak intensity agrees qualitatively with the experimental results of Fig. 5. The energy shift seen in Fig. 3(c) and (d) would be explained by multi-plasmon of n =8 and 9. Furthermore, the correlation between successive plasmon excitations would keep the multi-plasmon peak sharp, in contrast with the broadening of the multi plasmon peaks for electron impact[14,15], where no correlation between successive plasmon excitations exists. The model based on the exclusive excitation hypothesis appears to explain qualitatively the present experimental results. The validity of this hypothesis should be investigated in more details.

5 Summary

We have observed new energy loss peaks around 210 and 400 eV for 100keV H^+ transmitted through thin carbon films. Though the origins of these peaks are not well understood at the moment, the multi-plasmon excitation mechanism based on the exclusive excitation hypothesis seems to be responsible for the 210 eV peak. The model calculation is found to reproduce the observed results reasonably well. Further experimental and theoretical investigations are under way.

We are grateful to Drs. Y. Yamazaki and K. Kuroki who supplied us carbon films, for helpful discussions, to Dr. A. Sagara for elastic recoil detection measurement, to Dr. M. Iseki for electron impact measurement and to Prof. N. Itoh for valuable discussions.

This work has been partly supported by the co-operative program of National Institute for Fusion Science.

References

[1] D. Pines, "Elementary Excitations in Solids: (Benjamin Inc,1964).

[2] H. Reather, "Excitation of Plasmons and Interband Transitions" (Springer-Verlag, 1980).

[3] T. Oku, J. Kanasaki, N. Matsunami, N. Itoh, K. Matsuda and M. Aoki, Nucl. Instrum. & Method. B15 (1986) 142.

[4] N. Matsunami, Scanning Microscopy 1 (1987) 1593.

[5] N. Matsunami, K. Kitoh and M. Gotoh, "Ion Beam Interactions in Solids" eds. T. Mikumo, M. Mannami, K. Masuda, R. Shimizu and F. Fujimoto (1988) p337.

[6] J. F. Ziegler, J. P. Biersack and U. Littmark, "The Stopping and Range of Ions in Solids" (Pergamon Press, New York, 1985).

[7] P. Bauer, Nucl. Instrum. & Method. B45 (1990) 673.

[8] N. Matsunami and K. Kitoh, Nucl. Instrum. & Method.(1991, in print)

[9] P. V. Vavilov, Soviet Physics JETP 5 (1957) 749.

[10] P. Sigmund and K. B. Winterbon, Nucl. Instrum. & Methods B12 (1985) 1.

[11] T. Kaneko and Y. Yamamura, Phys. Rev. A33 (1986) 1653 and private communication.

[12] T. A. Carlson, C. C. Lu, T. C. Tucker, C. W. Nester Jr. and F. B. Malik, ORNL-4614 (1970).

[13] J. D. Garcia, R. J. Fortner and T. M. Kavanagh, Rev. Mod. Phys., 45 (1973) 111.

[14] A. W Blackstock, R. H. Ritchie and R. D. Birkhoff, Phys. Rev. 100 (1955) 1078.

[15] L. Marton, J. A. Simpson, H. A. Fowler and N. Swanson, Phys. Rev. 126 (1962) 182.

Table 1 Possible impurities having shells of binding energy U(eV) close to 210 eV. σ, Nσ and f are the calculated ionization cross section, ionization probability and necessary impurity fraction to give the intensity of 10^{-3} for 100 keV H^+ impact.

	U(eV)	σ ($\times 10^{-18}$ cm^2)	Nσ (λ=6 nm)	f=10^{-3}/Nσ (%)
B(1S)	196	0.87	0.057	1.7
C(1S)	290	0.23	0.015	—
S(2S)	226	0.57	0.038	2.7
Cl(2P)	210	2.2	0.145	0.7
Cl(2S)	268	0.29	0.019	

Figure captions

Fig. 1 Schematic of the experimental set-up. The materials used for the beam slits, deflector and etc. are given in the parentheses and ss denotes stainless steel.

Fig. 2 Energy loss spectrum for 100 keV H^+ without carbon film, showing the resolution, zero energy loss peak and flat background.

Fig. 3 Energy spectra of H^+ transmitted through thin carbon films: (a) and (c) for 100, and (b) and (d) for 120 keV. The solid lines around the energy loss of 1 keV are the asymmetric Gaussian fit to the data. The spectra around 1 keV indicated by crosses and open circles are obtained for as prepared sample and after bombardment of H^+ to a dose of ~0.1 $\mu C/mm^2$, respectively. The numbers are the half-width at half-maximum in eV. The solid lines around 210 eV are the single or double Gaussian fit to the data with the full-width at half-maximum indicated in the figure.

Fig. 4 RBS spectra of 2 MeV He on Be with (a) and without (b) C-film of 10 nm. Scattering angle is 160° with normal incidence.

Fig. 5 Intensity of 210 eV energy loss peak over the normal energy loss peak vs the film thickness. The dashed line shows the intensity oscillation with the period of λ_o.

Fig. 6 Calculated energy loss spectra for 100 keV H^+ in C film, with the film thickness of 6 nm (a), 6.2 nm (b), 6.5 nm (c) and 6.75 nm (d).

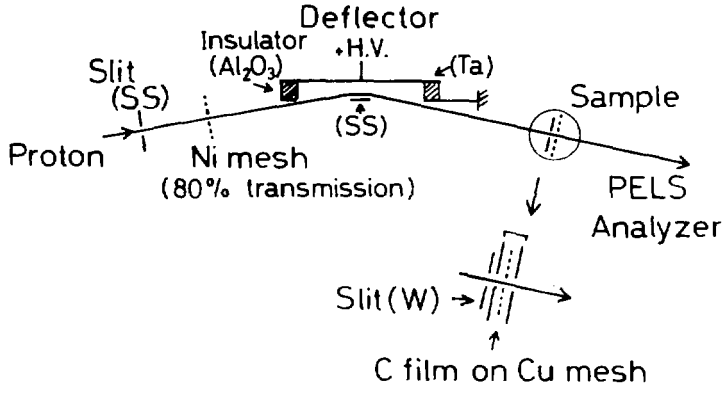
Deflector
Insulator
(Al2O3)
+H.V.
(Ta)
Slit
(SS)
(SS)
Sample
Proton
Ni mesh
(80% transmission)
PELS
Analyzer
Slit (W)
C film on Cu mesh

Fig. 1

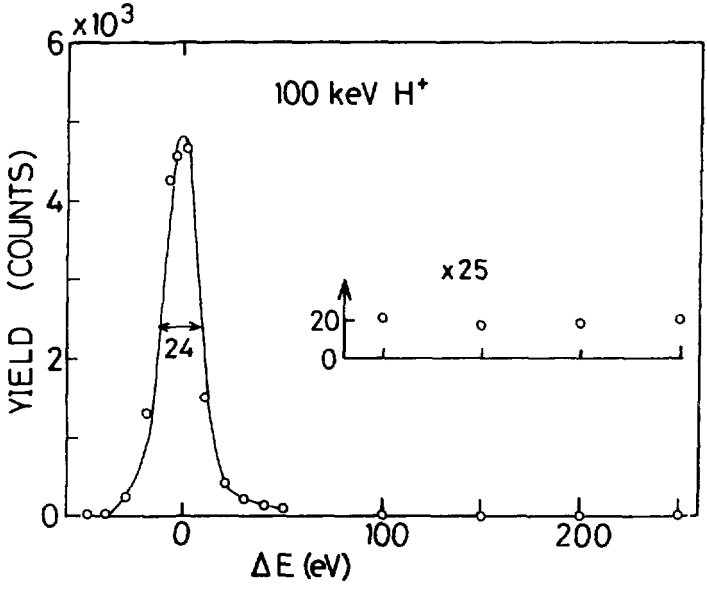
x10^3
6
4
2
0
100 keV H+
YIELD (COUNTS)
24
x25
20
0
0
100
200
ΔE (eV)

Fig. 2

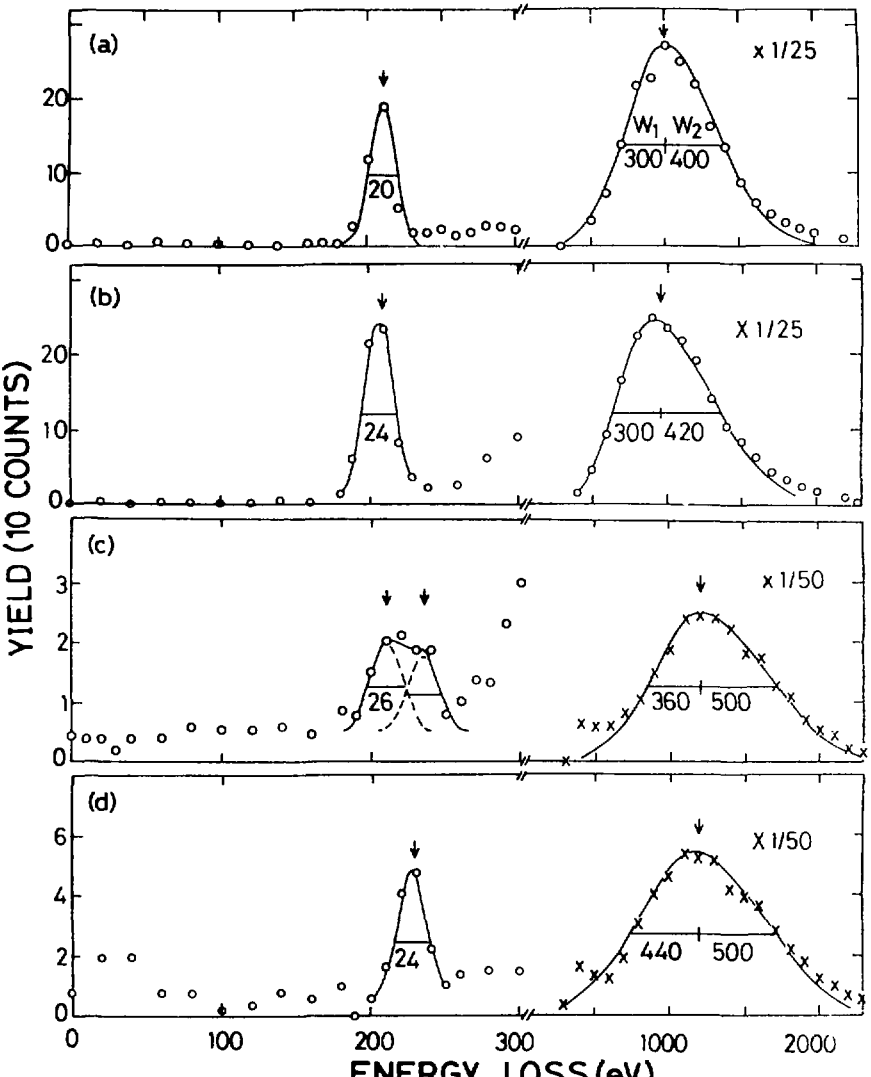
(a)
x 1/25
W1 W2
300 400
20
(b)
X 1/25
300 420
24
(c)
x 1/50
360 500
26
(d)
X 1/50
440 500
24
YIELD (10 COUNTS)
ENERGY LOSS (eV)
0
100
200
300
1000
2000

Fig. 3

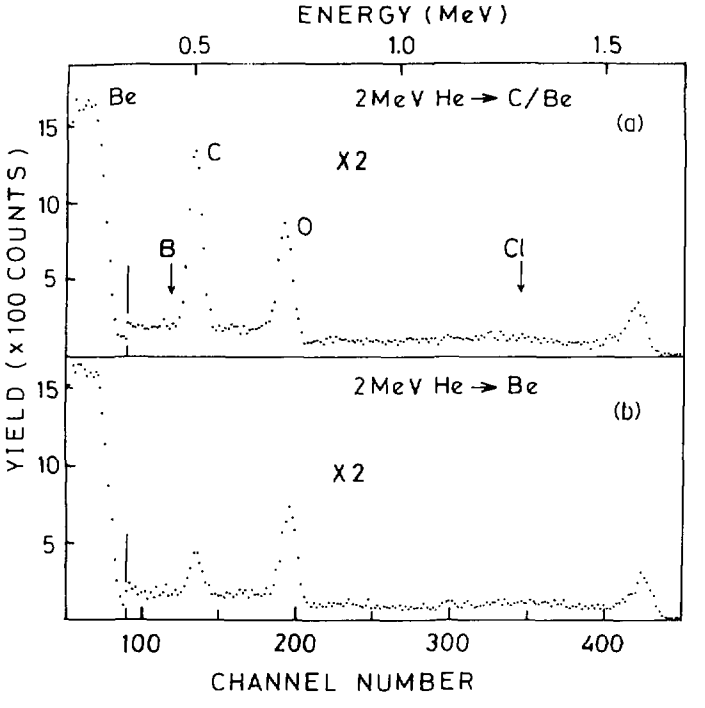
ENERGY (MeV)
0.5
1.0
1.5
Be
2MeV He → C/Be
(a)
C
X2
O
B
Cl
YIELD (x100 COUNTS)
15
10
5
2MeV He → Be
(b)
X2
100
200
300
400
CHANNEL NUMBER

Fig. 4

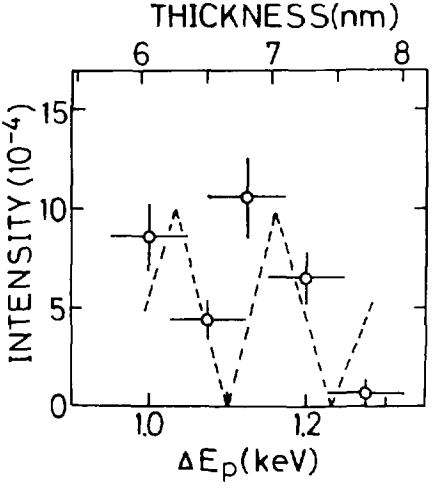
THICKNESS(nm)
6
7
8
INTENSITY (10^{-4})
15
10
5
0
1.0
1.2
ΔE_p(keV)

Fig. 5

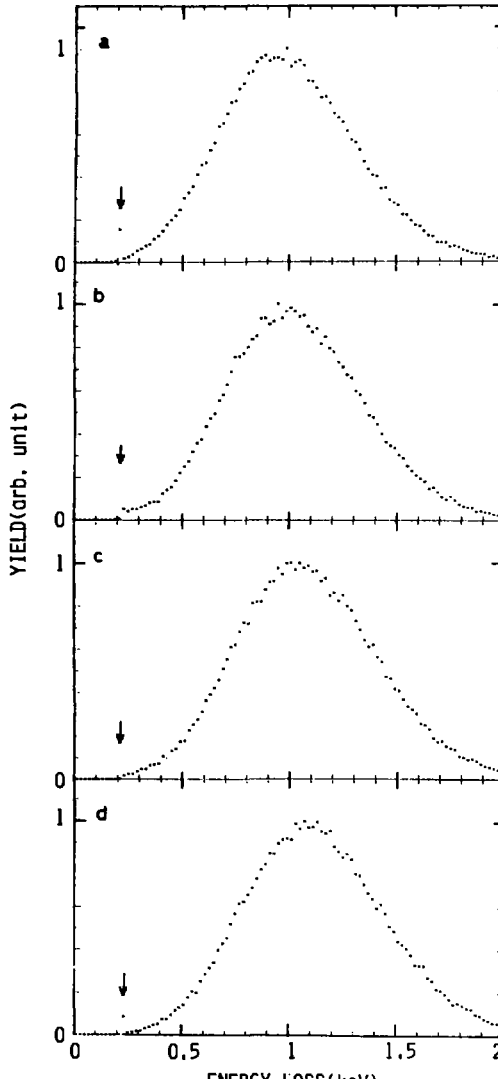

Fig. 6

Recen Issues of NIFS Series

NIFS-38 S.-I. Itoh and K. Itoh, *Modelling of Improved Confinements Peaked Profile Modes and H-Mode*; Sep. 1990

NIFS-39 O. Kaneko, S. Kubo, K. Nishimura, T. Syoji, M. Hosokawa, K. Ida, H. Idei, H. Iguchi, K. Matsuoka, S. Morita, N. Noda, S. Okamura, T. Ozaki, A. Sagara, H. Sanuki, C. Takahashi, Y. Takeiri, Y. Takita, K. Tsuzuki, H. Yamada, T. Amano, A. Ando, M. Fujiwara, K. Hanatani, A. Karita, T. Kohmoto, A. Komori, K. Masai, T. Morisaki, O. Motojima, N. Nakajima, Y. Oka, M. Okamoto, S. Sobhanian and J. Todoroki, *Confinement Characteristics of High Power Heated Plasma in CHS*; Sep. 1990

NIFS-40 K. Toi, Y. Hamada, K. Kawahata, T. Watari, A. Ando, K. Ida, S. Morita, R. Kumazawa, Y. Oka, K. Masai, M. Sakamoto, K. Adati, R. Akiyama, S. Hidekuma, S. Hirokura, O. Kaneko, A. Karita, T. Kawamoto, Y. Kawasumi, M. Kojima, T. Kuroda, K. Narihara, Y. Ogawa, K. Ohkubo, S. Okajima, T. Ozaki, M. Sasao, K. Sato, K.N. Sato, T. Seki, F. Shimpo, H. Takahashi, S. Tanahashi, Y. Taniguchi and T. Tsuzuki, *Study of Limiter H- and IOC- Modes by Control of Edge Magnetic Shear and Gas Puffing in the JIPP T-IIU Tokamak*; Sep. 1990

NIFS-41 K. Ida, K. Itoh, S.-I. Itoh, S. Hidekuma and JIPP T-IIU & CHS Group, *Comparison of Toroidal/Poloidal Rotation in CHS Heliotron/Torsatron and JIPP T-IIU Tokamak*; Sep. 1990

NIFS-42 T.Watari, R.Kumazawa, T.Seki, A.Ando, Y.Oka, O.Kaneko, K.Adati, R.Ando, T.Aoki, R.Akiyama, Y.Hamada, S.Hidekuma, S.Hirokura, E.Kako, A.Karita, K.Kawahata, T.Kawamoto, Y.Kawasumi, S.Kitagawa, Y.Kitoh, M.Kojima, T. Kuroda, K.Masai, S.Morita, K.Narihara, Y.Ogawa, K.Ohkubo, S.Okajima, T.Ozaki, M.Sakamoto, M.Sasao, K.Sato, K.N.Sato, F.Shimbo, H.Takahashi, S.Tanahashi, Y.Taniguchi, K.Toi, T.Tsuzuki, Y.Takase, K.Yoshioka, S.Kinoshita, M.Abe, H.Fukumoto, K.Takeuchi, T.Okazaki and M.Ohtuka, *Application of Intermediate Frequency Range Fast Wave to JIPP T-IIU and IIT-2 Plasma*; Sep. 1990

NIFS-43 K.Yamazaki, N.Ohyabu, M.Okamoto, T.Amano, J.Todoroki, Y.Ogawa, N.Nakajima, H.Akao, M.Asao, J.Fujita, Y.Hamada, T.Hayashi, T.Kamimura, H.Kaneko, T.Kuroda, S.Morimoto, N.Noda, T.Obiki, H.Sanuki, T.Sato, T.Satow, M.Wakatani, T.Watanabe, J.Yamamoto, O.Motojima, M.Fujiwara, A.Iiyoshi and LHD Design Group, *Physics Studies on Helical Confinement Configurations with l=2 Continuous Coil Systems*; Sep. 1990

NIFS-44 T.Hayashi, A.Takei, N.Ohyabu, T.Sato, M.Wakatani, H.Sugama, M.Yagi, K.Watanabe, B.G.Hong and W.Horton, *Equilibrium Beta Limit and Anomalous Transport Studies of Helical Systems*;

Sep. 1990

NIFS-45 R.Horiuchi, T.Sato, and M.Tanaka, *Three-Dimensional Particle Simulation Study on Stabilization of the FRC Tilting Instability*; Sep. 1990

NIFS-46 K.Kusano, T.Tamano and T. Sato, *Simulation Study of Nonlinear Dynamics in Reversed-Field Pinch Configuration*; Sep. 1990

NIFS-47 Yoshi H.Ichikawa, *Solitons and Chaos in Plasma*; Sep. 1990

NIFS-48 T.Seki, R.Kumazawa, Y.Takase, A.Fukuyama, T.Watari, A.Ando, Y.Oka, O.Kaneko, K.Adati, R.Akiyama, R.Ando, T.Aoki, Y.Hamada, S.Hidekuma, S.Hirokura, K.Ida, K.Itoh, S.-I.Itoh, E.Kako, A. Karita, K.Kawahata, T.Kawamoto, Y.Kawasumi, S.Kitagawa, Y.Kitoh, M.Kojima, T.Kuroda, K.Masai, S.Morita, K.Narihara, Y.Ogawa, K.Ohkubo, S.Okajima, T.Ozaki, M.Sakamoto, M.Sasao, K.Sato, K.N.Sato, F.Shinbo, H.Takahashi, S.Tanahashi, Y.Taniguchi, K.Toi and T.Tsuzuki, *Application of Intermediate Frequency Range Fast Wave to JIPP T-IIU Plasma*; Sep.1990

NIFS-49 A.Kageyama, K.Watanabe and T.Sato, *Global Simulation of the Magnetosphere with a Long Tail: The Formation and Ejection of Plasmoids*; Sep.1990

NIFS-50 S.Koide, *3-Dimensional Simulation of Dynamo Effect of Reversed Field Pinch*; Sep. 1990

NIFS-51 O.Motojima, K. Akaishi, M.Asao, K.Fujii, J.Fujita, T.Hino, Y.Hamada, H.Kaneko, S.Kitagawa, Y.Kubota, T.Kuroda, T.Mito, S.Morimoto, N.Noda, Y.Ogawa, I.Ohtake, N.Ohyabu, A.Sagara, T. Satow, K.Takahata, M.Takeo, S.Tanahashi, T.Tsuzuki, S.Yamada, J.Yamamoto, K.Yamazaki, N.Yanagi, H.Yonezu, M.Fujiwara, A.Iiyoshi and LHD Design Group, *Engineering Design Study of Superconducting Large Helical Device*; Sep. 1990

NIFS-52 T.Sato, R.Horiuchi, K. Watanabe, T. Hayashi and K.Kusano, *Self-Organizing Magnetohydrodynamic Plasma*; Sep. 1990

NIFS-53 M.Okamoto and N.Nakajima, *Bootstrap Currents in Stellarators and Tokamaks*; Sep. 1990

NIFS-54 K.Itoh and S.-I.Itoh, *Peaked-Density Profile Mode and Improved Confinement in Helical Systems*; Oct. 1990

NIFS-55 Y.Ueda, T.Enomoto and H.B.Stewart, *Chaotic Transients and Fractal Structures Governing Coupled Swing Dynamics*; Oct. 1990

NIFS-56 H.B.Stewart and Y.Ueda, *Catastrophes with Indeterminate Outcome*; Oct. 1990

NIFS-57 S.-I.Itoh, H.Maeda and Y.Miura, *Improved Modes and the Evaluation of Confinement Improvement*; Oct. 1990

NIFS-58 H.Maeda and S.-I.Itoh, *The Significance of Medium- or Small-size Devices in Fusion Research*; Oct. 1990

NIFS-59 A.Fukuyama, S.-I.Itoh, K.Itoh, K.Hamamatsu, V.S.Chan, S.C.Chiu, R.L.Miller and T.Ohkawa, *Nonresonant Current Drive by RF Helicity Injection*; Oct. 1990

NIFS-60 K.Ida, H.Yamada, H.Iguchi, S.Hidekuma, H.Sanuki, K.Yamazaki and CHS Group, *Electric Field Profile of CHS Heliotron/Torsatron Plasma with Tangential Neutral Beam Injection*; Oct. 1990

NIFS-61 T.Yabe and H.Hoshino, *Two- and Three-Dimensional Behavior of Rayleigh-Taylor and Kelvin-Helmholz Instabilities*; Oct. 1990

NIFS-62 H.B. Stewart, *Application of Fixed Point Theory to Chaotic Attractors of Forced Oscillators*; Nov. 1990

NIFS-63 K.Konn., M.Mituhashi, Yoshi H.Ichikawa,*Soliton on Thin Vortex Filament*; Dec. 1990

NIFS-64 K.Itoh, S.-I.Itoh and A.Fukuyama,*Impact of Improved Confinement on Fusion Research*; Dec. 1990

NIFS -65 A.Fukuyama, S.-I.Itoh and K. Itoh,*A Consistency Analysis on the Tokamak Reactor Plasmas*; Dec. 1990

NIFS-66 K.Itoh, H. Sanuki, S.-I. Itoh and K. Tani,*Effect of Radial Electric Field on α-Particle Loss in Tokamaks*; Dec. 1990

NIFS-67 K.Sato,and F.Miyawaki,*Effects of a Nonuniform Open Magnetic Field on the Plasma Presheath*; Jan.1991

NIFS-68 K.Itoh and S.-I.Itoh,*On Relation between Local Transport Coefficient and Global Confinement Scaling Law*; Jan. 1991

NIFS-69 T.Kato, K.Masai, T.Fujimoto,F.Koike, E.Källne, E.S.Marmar and J.E.Rice,*He-like Spectra Through Charge Exchange Processes in Tokamak Plasmas*; Jan.1991

NIFS-70 K. Ida, H. Yamada, H. Iguchi, K. Itoh and CHS Group, *Observation of Parallel Viscosity in the CHS Heliotron/Torsatron* ; Jan.1991

NIFS-71 H. Kaneko, *Spectral Analysis of the Heliotron Field with the Toroidal Harmonic Function in a Study of the Structure of Built-in Divertor* ; Jan. 1991

NIFS-72 S. -I. Itoh, H. Sanuki and K. Itoh, *Effect of Electric Field Inhomogeneities on Drift Wave Instabilities and Anomalous Transport* ; Jan. 1991

NIFS-73 Y.Nomura, Yoshi.H.Ichikawa and W.Horton, *Stabilities of Regular Motion in the Relativistic Standard Map*; Feb. 1991

NIFS-74 T.Yamagishi, *Electrostatic Drift Mode in Toroidal Plasma with Minority Energetic Particles*, Feb. 1991

NIFS-75 T.Yamagishi, *Effect of Energetic Particle Distribution on Bounce Resonance Excitation of the Ideal Ballooning Mode*, Feb. 1991

NIFS-76 T.Hayashi, A.Tadei, N.Ohyabu and T.Sato, *Suppression of Magnetic Surface Breading by Simple Extra Coils in Finite Beta Equilibrium of Helical System;* Feb. 1991

NIFS-77 N. Ohyabu, *High Temperature Divertor Plasma Operation*; Feb. 1991

NIFS-78 K.Kusano, T. Tamano and T. Sato, *Simulation Study of Toroidal Phase-Locking Mechanism in Reversed-Field Pinch Plasma*; Feb. 1991

NIFS-79 K. Nagasaki, K. Itoh and S.-I. Itoh, *Model of Divertor Biasing and Control of Scrape-off Layer and Divertor Plasmas*; Feb. 1991

NIFS-80 K. Nagasaki and K. Itoh, *Decay Process of a Magnetic Island by Forced Reconnection*; Mar. 1991

NIFS-81 K. Takahata, N. Yanagi, T. Mito, J. Yamamoto, O.Motojima and LHDDesign Group, K. Nakamoto, S. Mizukami, K. Kitamura, Y. Wachi, H. Shinohara, K. Yamamoto, M. Shibui, T. Uchida and K. Nakayama, *Design and Fabrication of Forced-Flow Coils as R&D Program for Large Helical Device*; Mar. 1991

NIFS-82 T. Aoki and T. Yabe, *Multi-dimensional Cubic Interpolation for ICF Hydrodynamics Simulation*; Apr. 1991

NIFS-83 K. Ida, S.-I. Itoh, K. Itoh and S. Hidekuma, *Density Peaking in the JFT-2M Tokamak Plasma with Counter Neutral Beam Injection* ; May 1991

NIFS-84 A. Iiyoshi, *Development of the Stellarator/Heliotron Research*; May 1991

NIFS-85 Y. Okabe, M. Sasao, H. Yamaoka, M. Wada and J. Fujita, *Dependence of Au⁻ Production upon the Target Work Function in a Plasma-Sputter Type Negative Ion Source*, May 1991

NIFS-86 N. Nakajima and M. Okamoto, *Geometrical Effects of the Magnetic Field on the Neoclassical Flow, Current and Rotation in General Toroidal Systems*, May 1991

NIFS-87 Sanae-I. Itoh, K. Itoh, A. Fukuyama, Y. Miura and JFT-2M Group, *ELMy-H mode as Limit Cycle and Chaotic oscillations in Tokamak Plasmas*, May 1991